Published in final edited form as:
Stem Cell Res. 2009 ; 3(2-3): 142–156. doi:10.1016/j.scr.2009.07.002.

Enhancement of Human Embryonic Stem Cell Pluripotency Through Inhibition of The Mitochondrial Respiratory Chain

S. Varum[1,3], **O. Momcilovic**[1,4], **C. Castro**[1,2], **A. Ben-Yehudah**[1,2], **J. Ramalho-Santos**[3,*], and **C. S. Navara**[5,*]

[1]Pittsburgh Development Center, Gynecology and Reproductive Sciences, University of Pittsburgh School of Medicine, Pittsburgh, Pennsylvania

[2]Department of Obstetrics, Gynecology and Reproductive Sciences, University of Pittsburgh School of Medicine, Pittsburgh, Pennsylvania

[3]Center for Neuroscience and Cell Biology, Department of Life Sciences, School of Science and Technology, University of Coimbra, Portugal

[4]Department of Human Genetics, Graduate School of Public Health, University of Pittsburg

[5]Biology Department, University of Texas, San Antonio

Abstract

Human embryonic stem cell pluripotency has been reported by several groups to be best maintained by culture under physiological oxygen conditions. Building on that finding, we inhibited complex III of the mitochondrial respiratory chain using Antimycin A or Myxothyazol to examine if specifically targeting the mitochondria would have a similar beneficial result for the maintenance of pluripotency. hESC's grown in the presence of 20nM Antimycin A maintained a compact morphology with high nuclear/cytoplasmic ratios. Furthermore, Real Time PCR analysis demonstrated that the levels of Nanog mRNA were elevated two fold in Antimycin A treated cells. Strikingly, Antimycin A was also able to replace bFGF in the media without compromising pluripotency, as long as autocrine bFGF signaling was maintained. Further analysis using low density quantitative PCR arrays showed that Antimycin A treatment reduced the expression of genes associated with differentiation possibly acting through a ROS-mediated pathway. These results demonstrate that modulation of mitochondrial function results in increased pluripotency of the cell population, and sheds new light on the mechanisms and signaling pathways modulating hESC pluripotency.

Keywords

human embryonic stem cells; pluripotency; mitochondria; mitochondrial complex III; Antimycin A

*Co-Corresponding Authors (christopher.navara@utsa.edu; jramalho@ci.uc.pt).

Introduction

The mechanisms underlying the maintenance of hESC self renewal and pluripotency are complex and poorly understood. Furthermore, the mechanisms by which hESC and mouse embryonic stem cells (mESC) maintain pluripotency differ. Both Leukemia Inhibitory Factor (LIF) and Bone Morphogenetic Protein 4 (BMP 4) play important roles in the maintenance of mESC self renewal via activation of Stat3 [1-3]. Conversely, LIF is not sufficient to maintain pluripotency of hESC [4] and addition of BMP 4 to the culture media results in rapid differentiation [5]. Instead, the combined actions of basic Fibroblast Growth Factor (bFGF, FGF2) and TGFβ/Activin/Nodal signaling pathways are believed to be critical to hESC self renewal. Nearly all formulations for the routine culture of hESC include exogenous bFGF, demonstrated to increase the cloning efficiency of hESC maintained in serum free conditions [6]. When added at high concentrations bFGF supports hESC self renewal in feeder-free conditions in the presence [7-8] or absence of conditioned media [8]. Several studies have also shown that the combined activities of Noggin and bFGF maintain hESC self renewal in the absence of conditioned medium due to the suppression of BMP activity [9-10]. Furthermore, Activin or Nodal appear to cooperate with bFGF to maintain hESC pluripotency in chemically defined media [11].

In addition to media constituent requirements Ezashi et al. [12] demonstrated that culture of hESC under low oxygen (O_2) tension (5%) reduced the appearance of spontaneous differentiation. This may be the normal physiological state, as early-stage mammalian embryos also develop under low O_2 concentrations (1.5%-5.3%) until they implant in the uterine endometrium, when O_2 levels increase with vascularization [13]. When cultured under low O_2 tension, mammalian cells decrease ATP production via oxidative phosphorylation in the mitochondria and increase glycolytic functions in order to meet energy demands. Studies of mitochondrial number and morphology in hESC have demonstrated that undifferentiated hESC have relatively few mitochondria in the cytoplasm and these mitochondria have few christae, an indication of immature morphology [14-16]. As hESC differentiate the number of mitochondria with a mature morphology increases, concomitant with the ATP levels produced by oxidative phosphorylation [16]. Taken together, these results suggest that inhibition of mitochondrial function may prevent differentiation, and thus modulate the maintenance of pluripotency.

In this study we tested this hypothesis by specifically inhibiting complex III of the mitochondrial respiratory chain using Antimycin A, an antibiotic isolated from *streptomyces sp*. Antimycin A specifically blocks the flow of electrons from semiquinone to ubiquinone in the quinone cycle of complex III, thus disrupting the proton gradient across the inner membrane of mitochondria and preventing O_2 consumption at complex IV as well as ATP formation. Complex III is also known to be a source of Reactive Oxygen Species (ROS) production in the cell; predominantly superoxide anion (O_2^-), which when produced in moderate amounts activates hypoxic signaling pathways in the cell. Consequently, complex III is considered the O_2 sensor of the cell [17-18]. Antimycin A treatment simultaneously decreases ATP production via oxidative phosphorylation and increases ROS formation.

Materials and Methods

Human embryonic stem cell culture

WA07 cells (WiCell) were cultured under normoxic conditions (21% O_2 and 5% CO_2) in Knockout medium containing 80% Knockout Dulbecco's modified Eagle's medium (DMEM) (Invitrogen, Carslbad, CA) supplemented with 20% Knockout Serum Replacer (Invitrogen), 1mM L-glutamine, 4ng/ml basic human recombinant FGF and 0.1mM MEM non essential amino acids, 50μg/ml penicillin, and 50μg/ml streptomycin (all from Invitrogen, Carlsbad,

CA). Cells were passaged manually (day 0) using a pulled glass needle and then plated onto Mitomycin C inactivated mouse embryonic fibroblast feeder cells - MEF's (Specialty Media, Phillipsburgh, NJ). On day two, 20 nM Antimycin A (Sigma-Aldrich, St Louis, MO) was added and media was changed every other day and new drug was added. hESC culture on Matrigel (BD Biosciences) was performed as described previously [19] briefly, human knockout medium was conditioned in MEF's and a total of 8ng bFGF/ml was used to supplement the media. Matrigel was diluted according to manufacturer's instructions and was allowed to coat dishes for at least 30 min at room temperature before cells were added. In order to allow cells to plate, treatments were initiated at day two after scraping and fresh media and drugs were added every other day. MnTbap and PD173074 [20-21] were used at 50μM and 100nM, respectively.

Immunocytochemistry

Immunocytochemistry (ICC) for the standard pluripotency markers: Oct-4, Nanog and SSEA-4 was assessed as previously described [22]. Only cells in which Oct-4 was localized in the nucleus were considered positive for this marker, whereas cytoplasmatic localization was considered as negative.

RNA extraction, RT PCR and TaqMan Low Density Arrays

Total RNA extraction and PCR mixtures were prepared as previously described [23]. Real Time PCR was performed using an ABI Prism 7700 (Applied Biosystems Incorporated, Foster City, CA). Taqman gene expression assays (Applied Biosystems) were used for Nanog, Oct-4 and β actin. Water and no RT samples were used as negative controls, all samples were run in triplicate. The TaqMan® Array human stem cell Pluripotency Panel (Applied Biosystems) was used following manufacturer's instructions. Nine (FGF5, KRT1, GCM1, HBB, WT1, GCG, INS, IPF1, MYF5) genes were excluded from our analysis due to very poor amplification in any sample. mRNA fold changes were calculated using the -ΔΔCt method and normalized using β actin expression as endogenous control.

Western Blotting

hESC were collected manually in PBS and pelleted. Total protein extract was collected using RIPA buffer (Sigma) supplemented with 1mM PMSF. Protein quantification was carried out using the Bradford assay (Bio Rad laboratories Inc, CA) and 10 μg of protein was separated by 12% SDS-PAGE. Primary antibodies used: Nanog (Kamiya Biomedical Company) and Oct-4 (Santa Cruz Biotechnology). ECL Advance Western Blot Detection kit (Amersham Biosciences, Piscataway, NJ) was used for detection.

Teratoma Formation

hESC treated for prolonged periods of time with 20nM of Antimycin A either in the presence or in the absence of bFGF were injected into the testis of non-obese diabetic/severe combined immune deficient (NOD/SCID) mice. Three mice were injected per experiment as previously described [24].

Apoptosis/Necrosis assay

hESC were maintained on Matrigel and treated with Antimycin A as previously described and Apoptosis/Necrosis rates were detected using Annexin V/ PI apoptosis detection kit (BD Biosciences) following manufacturer's instructions. Briefly, cells were washed with PBS, dissociated with Accutase followed by two washes in cold (4°C 1×10^6 cells were resuspended in 100μl of binding buffer and 5μl of both Annexin V and PI were added. The mixture was incubated for 15 min at 25°C in the dark followed by the addition of 400μl binding buffer. Labeled cells were analyzed by flow cytometry (BD LSR II, BD Biosciences).

Measurement of hESC proliferation

hESC proliferation was determined by BrdU (Roche) incorporation into the genomic DNA during the S phase of the cell cycle. hESC maintained on Matrigel were treated with Antimycin A as previously described. At day six after plating hESC were incubated in medium containing BrdU for three hours and washed three times with PBS. Cells were fixed and incorporated BrdU was detected with Anti-BrdU according to manufacturer's instructions. Cells were imaged by confocal microscopy and at least 2500 cells were counted to determine number of cycling cells.

ATP measurement by HPLC

hESC were maintained on Matrigel and Antimycin A treated as previously described. Intracellular adenine nucleotides (ATP, ADP and AMP), were determined as previously described [25]. In brief, adenine nucleotides were extracted with 0.6 M Perchloric acid supplemented with 25 mM EDTA-Na. Cell supernatants were neutralized with 3M KOH in 1.5M Tris followed by centrifugation. Supernatants were assayed by high-performance liquid chromatography (HPLC). The detection wavelength was 254nm, and the column was a Licophesfere100 RP108 5μM (Merk). Adenylate Energy Charge was calculated according to the following formula: ATP+0.5×ADP/(ATP+ADP+AMP).

Lactate Dehydrogenase (LDH) activity

Lactate Dehydrogenase activity was determined using the QuantiChrom Lactate Dehydrogenase Kit (Bio Assay Systems, CA) following manufacturer's instructions. Cells were mechanically dissociated and lysed in 100mM potassium phosphate containing 2mM EDTA buffer, centrifuged and the resulting supernatants were assayed using the working reagent. Optical density was read at 565nm immediately after the mixture of the sample and the working reagent, and also 25min after addition. LDH activity was determined based on the following formula: LDH activity = $43.68 \times (OD_{S25} - OD_{S0})/(OD_{calibrator} - OD_{H2O}) \times$ dilution factor.

Superoxide anion detection by MitoSox Red

hESC were maintained on Matrigel for 7 days and treatments (Antimycin A and /or MnTbap) were initiated at day two after scraping. Fresh media and drugs were added every other day. On day seven, cells were washed with PBS and dissociated with Accutase followed by two washes in PBS. Superoxide was detected using MitoSox Red (Invitrogen). Cells were suspended in media and incubated with 2.5μM of MitoSox Red for 30 min at 37°C followed by one wash in PBS and subsequent analysis by Flow cytometry.

Statistical Analysis

Means and Standard Error of the Mean were calculated and statistically significant differences were determined by paired t-test, Chi-Square test, or One-Way ANOVA followed by Dunnett's Multiple Comparison test. n refers to sample size. Significance was determined at $p < 0.05$.

Results

Antimycin A (20nM) was added 48 hours after passaging to hESC cultures (WA07) growing on MEF's in standard culture media, and this treatment was maintained for 5 days (Fig. 1). hESC grown under these conditions maintained a typical compact morphology with high nuclear-cytoplasmic ratio and colonies with well-defined borders, comparable to those in control cells (Fig. 1d). To quantify the levels of pluripotency, we used Real Time PCR for the well characterized pluripotency transcription factors Nanog and POU5F1 (also known as Oct-4). hESC treated with Antimycin A showed a two fold increase in Nanog mRNA levels

compared with control cells (Fig. 1a, $p<0.01$, n= 6). Oct-4 mRNA levels were not statistically different (Fig. 1a). Similar results were obtained with the complex III inhibitor, Myxothiazol, used at a concentration of 20 nM (data not shown).

To determine if the effects observed after addition of Antimycin A to the culture media were sustained or only transient, hESC were maintained for several passages (1-2 months) in the presence of Antimycin A. hESC grown under these conditions maintained good morphology throughout and maintained a two-fold elevation of Nanog mRNA ($p<0.05$, n=3) relative to controls. Again, Oct-4 mRNA levels were not significantly different from controls (Fig. 1a). Western blot analysis of these extended treatment cells showed that Nanog protein levels were also increased in Antimycin A treated cells (Fig. 1b); Oct-4 protein levels were not significantly different between treatments (Fig. 1c). To ensure that prolonged Antimycin A treatment did not negatively impact the pluripotent phenotype, we characterized these cells by ICC for the pluripotency markers Oct-4, Nanog, and SSEA-4. Nanog and Oct-4 were both found in the nucleus of Antimycin A treated cells, and the cell surface marker SSEA-4 labeled colonies (Fig. 1d) similar to control cells.

To determine if Antimycin A treated cells retained the potential to differentiate *in vivo*, we injected hESC treated with Antimycin A for 9 passages into NOD/SCID mice to test their ability to form teratomas. Similar to hESC maintained under standard conditions (not shown), Antimycin A treated cells were able to form teratomas exhibiting tissues of all three germ layers (Fig. 1e), including gastrointestinal tissue (endoderm), cartilage (mesoderm) and neuro ganglia (ectoderm). Finally, cells grown for extended periods (19 passages) in the presence of Antimycin A also maintained a stable 46 XX karyotype (data not shown).

To exclude the possibility that the effect of Antimycin A on Nanog expression was due to an increase in cell survival of pluripotent stem cells relative to differentiated cells, the levels of Annexin V/PI positive cells were determined by flow cytometry (Fig. 2 a-c). There was no statistically significant difference in the percentage of viable cells between Control (83.25 ±2.15, Fig. 2a, c) and Antimycin A (81.2±9.9, Fig. 2b, c) treated cells. Based on these results Antimycin A does not appear to affect cell survival.

In addition, proliferation of hESC was determined by BrdU incorporation into genomic DNA during S phase of the cell cycle (Fig.2 d-e). No statistically significant difference was observed in the percentage of cells that incorporate BrdU between control and Antimycin A treated cells. In combination with the above results, Antimycin A does not seem to affect cell death or proliferation of hESC.

As discussed above, bFGF is a well described factor important in the maintenance of pluripotency in hESC, even supporting pluripotency in the absence of feeder cells or conditioned media when present at high concentrations [9-10]. In order to better understand the beneficial effect of Antimycin A we cultured hESC on mouse feeders for 7 days using different combinations of Antimycin A and bFGF and assayed Oct-4 expression by ICC. Colonies were divided into three categories according to the pattern of Oct-4 expression and quantified: totally positive colonies in which the majority of cells were positive for Oct-4 (Fig. 3a bottom left); partially positive colonies containing a significant quantity of both positive and negative cells (Fig. 3a bottom center); and negative colonies in which the majority of cells were negative for Oct-4 (Fig. 3a bottom right). At least 200 colonies were counted per treatment. As expected, removal of bFGF from the media resulted in a significant decrease in the number of totally positive colonies and an increase in the number of partially positive colonies (Fig.3b; $p<0.001$), confirming the importance of this growth factor in the maintenance of healthy hESC colonies. Interestingly, when Antimycin A was added to culture media lacking bFGF the number of totally positive colonies (65.9% vs. 67.0%) and partially positive colonies

(33.3% vs. 32.6%) was indistinguishable from standard culture conditions (Fig. 3b), suggesting that addition of Antimycin A maintains Oct-4 expression levels in culture conditions lacking bFGF. Surprisingly, the addition of both Antimycin A and bFGF to the culture increased the number of totally positive colonies (86.8% vs 67.07%, $p<0.001$). This answer to this apparent contradiction is unknown but several factors may be involved. Firstly, western blotting and Real Time PCR are unbiased quantitative analyses that probe an entire population of cells, while ICC as carried out here was inherently qualitative in terms of signal intensity, colony size and colony heterogeneity (i.e., more or less positive cells in a colony), all of which could have played a role. Furthermore, subcellular localization of Oct-4 should also be considered. It is understood that during early differentiation of hESC Oct-4 localizes primarily in the cytoplasm instead of the nucleus, as is observed with undifferentiated hESC. During human development Oct-4 is first observed cytoplasmically before localizing to the nucleus in the inner cell mass [53]. In this case cells in which Oct-4 localizes to the cytoplasm will be counted as negative in our ICC analysis but would still be positive by western blotting. Subcellular localization of Oct-4 may thus be a better assay of pluripotency than total cellular protein. Importantly, when performing double labeling experiments for both Oct-4 and Nanog, the most striking effect of Antimycin treatment within single colonies was an increase of Oct-4+/Nanog + cells (97% vs. 70%) at the expense of the Oct-4+/Nanog-subpopulation (0.4% vs. 23%). Finally, we performed Real Time PCR for Nanog in both WA07 (Fig.3c) and WA09 (Sup Fig. 1, carried out in a separate facility) for the conditions above. We observed that both cell lines are responsive to bFGF withdrawal demonstrated by a decrease in Nanog expression. In both cell lines Antimycin A maintains Nanog expression upon bFGF withdrawal, suggesting that this effect is not related to the particular characteristics of one hESC line.

One possible explanation for these results is that Antimycin A induces bFGF secretion by feeders and/or hESC. In order to address this point, bFGF concentration in the culture media was measured by ELISA (Sup Fig. 2). No bFGF secretion by mitomycin inactivated MEF's was detected. The bFGF initially present in the media (4ng/ml), was rapidly degraded/ processed by the cells, as demonstrated in media concentrations of 65.92±5.01 pg/ml and 24.41 ±3.58 pg/ml after 6 hr or 24 hr of culture, respectively (Sup Fig. 2 a). These results are in accordance with the findings of Eiselleova et al.[26] that showed, in contrast to human feeders, MEFs do not produce bFGF. Antimycin A treatment does not promote bFGF secretion by the MEFs as media concentrations are indistinguishable from controls (59.04± 3.94pg/ml and 27.31± 7.89pg/ml) after 6 hr and 24 hr of culture, respectively. In contrast to MEFs, hESCs appear to secrete bFGF into the media, since concentrations of 64.40±36.72 pg/ml of bFGF were detected after 24 hr of culture in media not supplemented with bFGF (Supp Fig.2b). These results are in accordance with the findings of Dvorak et al.[27]. bFGF production by hESCs was not affected by Antimycin A treatment. These results indicate the effect of Antimycin A on pluripotency was not due to an increase in bFGF secretion by the feeders or by hESC themselves.

These findings raise questions regarding the involvement of the bGF pathway in this effect. To address this issue we used the bFGF receptor inhibitor PD173074 [20]. hESC were maintained on Matrigel for 7 days in different combinations of bFGF, PD173074 and Antimycin A (Fig. 3d). Similar to what we observed for hESC cultured on feeders, bFGF removal reduced Nanog expression (1.6 fold decrease) when compared to control cells (bFGF alone). Moreover, the addition of PD173074 promoted a significant decrease in Nanog and Oct-4 expression when compared to control cells (2.8 and 2.1 fold decrease, respectively). These results are in accordance with the findings of Dvorak et al.[28] who demonstrated a crucial role for the autocrine bFGF signaling pathway in the maintenance of hESCs self-renewal. Treatment with Antimycin A in the absence of bFGF maintained Nanog and Oct-4 mRNA expression at similar levels to controls; however, the expression of these markers decreased significantly upon the addition of PD173074 (1.8 and 1.96 fold decrease for Nanog

and Oct-4, respectively). Interestingly, the decrease in Nanog mRNA levels after the addition of PD173074 was less accentuated in the presence of Antimycin A, perhaps suggesting that Antimycin A functions through a different pathway than bFGF. These results indicate that, although Antimycin A can maintain the expression levels of pluripotency markers in absence of exogenous bFGF, it cannot maintain pluripotency when the endogenous bFGF pathway is inhibited, reinforcing the importance of the autocrine bFGF signaling pathway. Additionally, since Antimycin A mitigated the effects of both exogenous bFGF removal and the inhibition of the endogenous bFGF pathway by PD173074, it is likely that Antimycin A acts in a pathway separate from bFGF.

To determine if cells treated with Antimycin A remain pluripotent in the absence of bFGF for prolonged periods of time, hESC were treated with Antimycin A in knockout media without bFGF for periods greater than one month. The best colonies in all conditions were manually passaged every 7 days. hESC maintained under these conditions had a similar morphology to control cells, including tightly packed cells in colonies with well defined borders (Fig. 3e). Immunocytochemical analysis demonstrated that these cells express the pluripotency markers Nanog, Oct-4 and SSEA-4 in similar patterns to control cells (Fig. 3e). We also evaluated the capacity of these cells to differentiate *in vivo*. Antimycin A treated cells grown in the absence of exogenous bFGF (33 passages) generated teratomas exhibiting tissues from all three germ layers (Fig. 3f). These cells maintained a stable 46XX karyotype after prolonged culture (19 passages, data not shown).

To further investigate the role of Antimycin A treatment on gene expression we used the TaqMan® Low Density Array human stem cell Pluripotency Panel. These arrays contain 90 genes involved in maintenance of pluripotency or promotion of differentiation, along with 6 endogenous control genes [29]. We maintained hESC in different combinations of Antimycin A and bFGF for more than 20 passages, and analyzed mRNA levels by Real Time PCR. Among the genes analyzed were Nanog [30-31], POUF51 [32] and TDGF1 [33], all critical for the maintenance of pluripotency. Consistent with our findings using single gene assays, treatment with Antimycin A in the presence of bFGF resulted in a statistically significant two fold increase in Nanog expression, when analyzed with the low density array (Fig. 4a;n=3; $p<0.01$). This difference was maintained in the absence of bFGF ($p<0.01$). TDGF1 was also significantly elevated after treatment with Antimycin A (1.8-fold increase; $P<0.01$), while POU5F1 was elevated but not significantly. Both TDGF1 and POU5F1 were elevated in the absence of bFGF but did not rise to the level of significance. The other four pluripotency genes (SOX2, DMNT3B, GABRB3 and GDF3) on the array were not elevated and, surprisingly, removal of both Antimycin A and bFGF did not significantly reduce expression levels of any of these genes (Fig. 4a, heatmap) When 32 genes correlated with pluripotency were examined, several genes were found to be amplified (Fig. 4b, heatmap), including EBAF, LEFTB and NODAL, but several others decreased with Antimycin A treatment including GBX2 and CRABP2. To compare these genes as a group across treatments, we averaged the fold changes across all 32 genes. No significant differences in the expression of these pluripotency correlated genes were observed between any treatments (Fig. 4b).

We also studied the expression of genes involved in differentiation. These genes were grouped according to their participation in endoderm (Fig. 5a), mesoderm (Figure 5b), trophoblast (Fig. 5c), or ectoderm (Fig. 5d) differentiation and averaged as above. Antimycin A treatment in the absence of bFGF resulted in no statistical differences in the expression of differentiation genes in comparison to control cells (Fig. 5a-d). The addition of Antimycin A in the presence of bFGF reduced the expression of differentiation genes in all categories (Fig. 5a-c), although only the decrease in ectoderm related genes was statistically significant (Fig. 5d, $p<0.01$, n=3). These results are in accordance with the findings of Vallier et al.[34] who reported that Nanog overexpression prevents neuroectoderm differentiation. In contrast to the pluripotency genes

whose expression did not change after withdrawal of bFGF and Antimycin A, endoderm, trophoblast and mesoderm genes were all significantly higher in the absence of these compounds (Fig. 5a-c; $p<0.01$, $n=3$). Only the ectodermal genes were unchanged in the absence of bFGF and Antimycin A (Figure 5d). This last result is in accordance with Stern et al. [35] who reported that bFGF plays a crucial role in neuroectoderm specification in amphibian and chick embryos.

Antimycin A traditionally stimulates a shift in the metabolism from oxidative phosphorylation to glycolysis (due to lower mitochondrial function) and promotes an increased superoxide generation at complex III (due to a lack of normal electron flow to oxygen, and thus the "leaking" of high-energy electrons from the transport chain). In order to determine if Antimycin A treatment has the same effect in hESC, the levels of adenine nucleotides (ATP, ADP and AMP) were measured by HPLC in Control and Antimycin A treated hESC. No significant differences in the adenylate pool or adenylate charge were observed between the two conditions (Fig.6 a-b). Lactate Dehydrogenase (LDH) is an enzyme that converts pyruvate, the final product of glycolysis, to lactate when a decline in O_2 availability or impaired ATP production by mitochondria forces the cell into anaerobic metabolism, or when aerobic glycolysis is favored, as is the case in some cancers. Antimycin A treated cells showed an increase of approximately 40% in the rates of LDH activity (Fig.6 c). These results indicate that Antimycin A induces a shift in the metabolism towards glycolysis similar to what is observed in other cell types. However, hESC cultured in the presence of Antimycin A maintained ATP levels consistent with untreated cells.

As mentioned above, Antimycin A increases the production of ROS in cells. To determine the effect of Antimycin A on mitochondrial superoxide anion production in hESC, we used MitoSox Red (Fig.7). Cells treated with 20 nM Antimycin A showed an increase of approximately 61%±20.7% in the number of positive cells for MitoSox Red when compared with control cells, as monitored by flow cytometry. This effect was dose dependent as treatment of hESC with 2 μM of Antimycin A increased the number of positive cells approximately 250% ±16.3%. This effect was counteracted by the addition of MnTbap, a cell permeable Superoxide Dismutase (SOD) mimetic which acts as a scavenger specifically targeting superoxide. Treatment with 50μM MnTbap eliminated the effect of treatment with 20nM Antimycin A. MnTbap was also able to reduce the number of positive hESC under control conditions (Fig. 7a, b).

Reactive oxygen species are important signaling molecules within the cell. To address whether the effect of Antimycin A on pluripotency is mediated by ROS cells were maintained in different combinations of Antimycin A and MnTbap and Real Time PCR for Nanog was performed (Fig. 7c). MnTbap was able to partially abrogate the Antimycin A stimulated increase in Nanog expression, although no significant differences were observed between control and MnTbap treated cells. These results suggest that Superoxide anion generated at complex III is at least partially responsible for the effect of Antimycin A on Nanog expression.

Discussion

Studies have demonstrated that hESC cultured under low oxygen tension (1.5-5%) are better maintained in the undifferentiated state [12-36]. This suggests that a decrease in mitochondrial oxidative phosphorylation and an increase in ROS signaling under these conditions might be involved. We show here that this effect can be mimicked by directly inhibiting mitochondrial function in a way that is at least partially dependent on ROS formation. hESC treated with 20 nM Antimycin A maintained pluripotency not only as evidenced by immunocytochemical staining of the pluripotency markers but also as assayed by teratoma formation. Real Time PCR and Western Blot analysis demonstrated that Antimycin A treated hESC had elevated

levels of both Nanog mRNA and protein. While a similar increase was observed for TDGF1 mRNA expression, no significant differences were observed for Oct-4 protein or mRNA. These results can best be explained by considering that, unlike the case for Oct-4, overexpression of Nanog is beneficial for the maintenance of pluripotency, namely preventing neuroectoderm differentiation induced by FGF signaling [33]. Others have shown that overexpression of Nanog allows culture in the absence of feeders [37] and circumvents the need for both TGFb and FGF signaling in the maintenance of pluripotency [38]. In contrast Oct- 4 levels must be kept within defined ranges in order to maintain self-renewal of both mouse and human ESCs, as overexpression results in upregulation of markers involved in endoderm and mesoderm specification of both cell types [39-40] while, conversely, RNA interference targeting Oct-4 can trigger trophectoderm differentiation [41-43]. Additionally, Pan et al.[44] demonstrated that a steady-state concentration of Oct-4 maintains Nanog expression, whereas an elevated concentration of Oct-4 suppresses Nanog expression. Therefore, while upregulation of Nanog is globally beneficial to the maintenance of pluripotency, upregulation of Oct-4 can be detrimental and maintenance of the status quo is appropriate for Oct-4 expression. Taking into account these findings it seems that Antimycin A does not increase Oct-4 expression above the steady-state present in pluripotent hESC.

Very few growth factors have been identified as being necessary or sufficient for maintenance of hESC pluripotency, though one leading candidate is bFGF [6-8]. As bFGF and Antimycin A both promote pluripotency, we were interested in determining if Antimycin A could maintain pluripotency in the absence of bFGF. Treatment with Antimycin A was able to alleviate the requirement for exogenous bFGF as there was no difference in the number of totally positive colonies between standard culture conditions and those including Antimycin A but lacking bFGF. Furthermore, Antimycin A was able to sustain Nanog expression upon bFGF removal in both WA07 and WA09 cell lines demonstrating that the effect is not ES line dependent. Antimycin A treatment failed to maintain pluripotency upon the inhibition of the endogenous bFGF pathway, indicating the requirement for the endogenous bFGF pathway in the maintenance of pluripotency. The observation that Antimycin A increases Nanog expression even when the endogenous pathway is suppressed suggests that Antimycin A works through a pathway other than bFGF. Taken together, our results suggest that bFGF and Antimycin A work through synergistic pathways to maintain pluripotency.

Cells cultured for several months in the presence of Antimycin A and absence of exogenous bFGF remained pluripotent as assessed by ICC and Teratoma formation. Furthermore, Low density Array analysis showed that Antimycin A treatment of hESC cultured in the absence of bFGF resulted in an elevated expression of Nanog mRNA and maintained the expression of differentiation genes at similar levels to those found in control cells.

Our findings can be explained in light of morphological and functional changes that mitochondria undergo during early mammalian development. In the oocyte, mitochondria are spherical with few christae, whereas between the zygote and the morula stage, mitochondria become more elongated [45]. At the blastocyst stage two distinct forms of mitochondria are present: mitochondria in the inner cell mass (ICM) are spherical and have low O_2 consumption, whereas those in the trophectoderm (TE) are elongated and have higher respiratory rates [46-47]. As hESCs are derived from the ICM, one should expect that they share these metabolic and morphological features. Indeed, it has been shown that undifferentiated hESC have few mitochondria with an immature morphology, and a greater reliance on glycolysis [14-16]. As hESC differentiate both the number of mitochondria with a mature morphology increases, as well as ATP production by oxidative phosphorylation [16].

Finally, our results indicate that ROS produced at complex III of the mitochondrial electron transfer chain are at least partially responsible for the Antimycin A effect on Nanog expression.

Mitochondrial ROS constitute the major source of ROS in the cells and are produced as side products of oxidative phosphorylation. The involvement of ROS in deleterious processes such as DNA damage, changes in the native structure of proteins, and lipidic peroxidation of membranes has long been recognized. More recently, however, it has been recognized that ROS can modulate various intracellular signaling pathways through covalent modifications (so called “redox signaling”) of target molecules, thereby inducing changes in cells that are important in many physiological and pathophysiological processes [48]. In addition, there is a growing body of evidence that there is an increase in ROS production following the addition of a various peptide growth factors to cells in culture, and that these ROS are a crucial component of downstream signaling. Our results demonstrate that Antimycin A increases superoxide generation at complex III and that capture of superoxide anion by MnTbap partially abrogates the effect of Antimycin A in Nanog expression, suggesting ROS as at least a partial modulator of Antimycin A effect on pluripotency. Superoxide anion can rapidly convert to other reactive species and therefore not be captured by MnTbap, thus continuing to signal, which might also explain why MnTbap does not completely eliminate the Antimycin A effect. This is in accordance with the reports of Carriere et al.[49] demonstrating that Antimycin A inhibited murine preadipocyte differentiation towards the adipocyte phenotype by increasing ROS formation at complex III. Indeed, several growth factor and cytokines such as bFGF and TGFb are known to induce H_2O_2 generation in different cell types [50]. Alternatively, the effect of Antimycin A in Nanog expression could be a synergistic action between ROS production and a shift in oxidative metabolism towards glycolysis, which we have also demonstrated to take place. This latter hypothesis is in accordance with findings of Chung et al.[51] who showed that during the *in vitro* process of mESC differentiation, Antimycin A inhibits oxidative phosphorylation and leads to a reduced appearance of beating cardiomyocytes. In addition, we cannot rule out the hypothesis that the effect of Antimycin A on Nanog expression could be partially mediated by changes in calcium homeostasis. Indeed, Spitkovsky et al.[52], demonstrated that, while Antimycin A blocked cardiomyocyte differentiation by acting on calcium signaling, and that the use of KCN (an inhibitor of complex IV of the mitochondrial respiratory chain) did not. Further work is required to pinpoint the exact mechanism(s) involved but our data provide the first evidence that modulation of mitochondrial function (probably acting through a ROS-dependent pathway) can influence the pluripotent state of hESC.

Supplementary Material

Refer to Web version on PubMed Central for supplementary material.

Acknowledgments

We would like to acknowledge the invaluable help of several of our colleagues including: Gerald Schatten for critical reading of the manuscript, discussion of the results and financial support. Carrie Redinger and Jody Mich-Basso for hESC culture and RT PCR, Dave McFarland for help generating the teratomas and John Ozolek for analysis of teratomas. Special thanks are due to Yuki Ohi and Miguel Ramalho-Santos (University of California, San Francisco) for invaluable assistance with experiments involving the WA09 cell line. We would also like to thank Ana Sofia Rodrigues, Andre Tartar, Dan Constantinescu and Charles Easley for critical reading of the manuscript. This work was supported by a grant from the National Institute of Child Health and Human Development, 1PO1HD047675 (to Gerald Schatten) and Fundacão para a Ciencia e Tecnologia (FCT) for scholarship support of S.V. J.-R.-S. was supported by a Fulbright Fellowship.

References

[1]. Matsuda T, Nakamura T, Nakao K, Arai T, Katsuki M, Heike T, Yokota T. STAT3 activation is sufficient to maintain an undifferentiated state of mouse embryonic stem cells. Embo J 1999;18 (15):4261–4269. [PubMed: 10428964]

[2]. Niwa H, Burdon T, Chambers I, Smith A. Self-renewal of pluripotent embryonic stem cells is mediated via activation of STAT3. Genes Dev 1998;12(13):2048–2060. [PubMed: 9649508]

[3]. Ying QL, Nichols J, Chambers I, Smith A. BMP induction of Id proteins suppresses differentiation and sustains embryonic stem cell self-renewal in collaboration with STAT3. Cell 2003;115(3):281–292. [PubMed: 14636556]

[4]. Daheron L, Opitz SL, Zaehres H, Lensch MW, Andrews PW, Itskovitz-Eldor J, Daley GQ. LIF/STAT3 signaling fails to maintain self-renewal of human embryonic stem cells. Stem Cells 2004;22(5):770–778. [PubMed: 15342941]

[5]. Xu RH, Chen X, Li DS, Li R, Addicks GC, Glennon C, Zwaka TP, Thomson JA. BMP4 initiates human embryonic stem cell differentiation to trophoblast. Nat Biotechnol 2002;20(12):1261–1264. [PubMed: 12426580]

[6]. Amit M, Carpenter MK, Inokuma MS, Chiu CP, Harris CP, Waknitz MA, Itskovitz-Eldor J, Thomson JA. Clonally derived human embryonic stem cell lines maintain pluripotency and proliferative potential for prolonged periods of culture. Dev Biol 2000;227(2):271–278. [PubMed: 11071754]

[7]. Rosler ES, Fisk GJ, Ares X, Irving J, Miura T, Rao MS, Carpenter MK. Long-term culture of human embryonic stem cells in feeder-free conditions. Dev Dyn 2004;229(2):259–274. [PubMed: 14745951]

[8]. Xu C, Rosler E, Jiang J, Lebkowski JS, Gold JD, O'Sullivan C, Delavan-Boorsma K, Mok M, Bronstein A, Carpenter MK. Basic fibroblast growth factor supports undifferentiated human embryonic stem cell growth without conditioned medium. Stem Cells 2005;23(3):315–323. [PubMed: 15749926]

[9]. Wang G, Zhang H, Zhao Y, Li J, Cai J, Wang P, Meng S, Feng J, Miao C, Ding M, Li D, Deng H. Noggin and bFGF cooperate to maintain the pluripotency of human embryonic stem cells in the absence of feeder layers. Biochem Biophys Res Commun 2005;330(3):934–942. [PubMed: 15809086]

[10]. Xu RH, Peck RM, Li DS, Feng X, Ludwig T, Thomson JA. Basic FGF and suppression of BMP signaling sustain undifferentiated proliferation of human ES cells. Nat Methods 2005;2(3):185–190. [PubMed: 15782187]

[11]. Vallier L, Alexander M, Pedersen RA. Activin/Nodal and FGF pathways cooperate to maintain pluripotency of human embryonic stem cells. J Cell Sci 2005;118(Pt 19):4495–4509. [PubMed: 16179608]

[12]. Ezashi T, Das P, Roberts RM. Low O2 tensions and the prevention of differentiation of hES cells. Proc Natl Acad Sci U S A 2005;102(13):4783–4788. [PubMed: 15772165]

[13]. Fischer B, Bavister BD. Oxygen tension in the oviduct and uterus of rhesus monkeys, hamsters and rabbits. J Reprod Fertil 1993;99(2):673–679. [PubMed: 8107053]

[14]. St John JC, Ramalho-Santos J, Gray HL, Petrosko P, Rawe VY, Navara CS, Simerly CR, Schatten GP. The expression of mitochondrial DNA transcription factors during early cardiomyocyte in vitro differentiation from human embryonic stem cells. Cloning Stem Cells 2005;7(3):141–153. [PubMed: 16176124]

[15]. Oh SK, Kim HS, Ahn HJ, Seol HW, Kim YY, Park YB, Yoon CJ, Kim DW, Kim SH, Moon SY. Derivation and characterization of new human embryonic stem cell lines: SNUhES1, SNUhES2, and SNUhES3. Stem Cells 2005;23(2):211–219. [PubMed: 15671144]

[16]. Cho YM, Kwon S, Pak YK, Seol HW, Choi YM, Park do J, Park KS, Lee HK. Dynamic changes in mitochondrial biogenesis and antioxidant enzymes during the spontaneous differentiation of human embryonic stem cells. Biochem Biophys Res Commun 2006;348(4):1472–1478. [PubMed: 16920071]

[17]. Chandel NS, McClintock DS, Feliciano CE, Wood TM, Melendez JA, Rodriguez AM, Schumacker PT. Reactive oxygen species generated at mitochondrial complex III stabilize hypoxia-inducible factor-1alpha during hypoxia: a mechanism of O2 sensing. J Biol Chem 2000;275(33):25130–25138. [PubMed: 10833514]

[18]. Guzy RD, Hoyos B, Robin E, Chen H, Liu L, Mansfield KD, Simon MC, Hammerling U, Schumacker PT. Mitochondrial complex III is required for hypoxia-induced ROS production and cellular oxygen sensing. Cell Metab 2005;1(6):401–408. [PubMed: 16054089]

[19]. Xu C, Inokuma MS, Denham J, Golds K, Kundu P, Gold JD, Carpenter MK. Feeder-free growth of undifferentiated human embryonic stem cells. Nat Biotechnol 2001;19(10):971–974. [PubMed: 11581665]

[20]. Mohammadi M, Froum S, Hamby JM, Schroeder MC, Panek RL, Lu GH, Eliseenkova AV, Green D, Schlessinger J, Hubbard SR. Crystal structure of an angiogenesis inhibitor bound to the FGF receptor tyrosine kinase domain. EMBO J 1998;17(20):5896–5904. [PubMed: 9774334]

[21]. Ying QL, Wray J, Nichols J, Batlle-Morera L, Doble B, Woodgett J, Cohen P, Smith A. The ground state of embryonic stem cell self-renewal. Nature 2008;453(7194):519–523. [PubMed: 18497825]

[22]. Navara CS, Redinger C, Mich-Basso J, Oliver S, Ben-Yehudah A, Castro C, Simerly C. Derivation and characterization of nonhuman primate embryonic stem cells. Curr Protoc Stem Cell Biol. 2007 Chapter 1:Unit 1A 1.

[23]. Navara CS, Redinger C, Mich-Basso J, Oliver S, Ben-Yehudah A, Castro C, Simerly C. Derivation and characterization of nonhuman primate embryonic stem cells. Curr Protoc Stem Cell Biol. 2007a Chapter 1: Unit 1A 1.

[24]. Navara, CS.; Redinger, C.; Mich-Basso, J.; Oliver, S.; Ben-Yehudah, A.; Castro, C.; Simerly, CR. Derivation and Characterization of Non-human Primate Embryonic Stem Cells. John Wiley and Sons; 2007.

[25]. Amaral S, Moreno AJ, Santos MS, Seica R, Ramalho-Santos J. Effects of hyperglycemia on sperm and testicular cells of Goto-Kakizaki and streptozotocin-treated rat models for diabetes. Theriogenology 2006;66(9):2056–2067. [PubMed: 16860381]

[26]. Eiselleova L, Peterkova I, Neradil J, Slaninova I, Hampl A, Dvorak P. Comparative study of mouse and human feeder cells for human embryonic stem cells. Int J Dev Biol 2008:353–363. [PubMed: 18415935]

[27]. Dvorak P, Hampl A. Basic fibroblast growth factor and its receptors in human embryonic stem cells. Folia Histochem Cytobiol 2005;43(4):203–208. [PubMed: 16382885]

[28]. Dvorak P, Dvorakova D, Koskova S, Vodinska M, Najvirtova M, Krekac D, Hampl A. Expression and potential role of fibroblast growth factor 2 and its receptors in human embryonic stem cells. Stem Cells 2005;23(8):1200–1211. [PubMed: 15955829]

[29]. Adewumi O, Aflatoonian B, Ahrlund-Richter L, Amit M, Andrews PW, Beighton G, Bello PA, Benvenisty N, Berry LS, Bevan S, Blum B, Brooking J, Chen KG, Choo AB, Churchill GA, Corbel M, Damjanov I, Draper JS, Dvorak P, Emanuelsson K, Fleck RA, Ford A, Gertow K, Gertsenstein M, Gokhale PJ, Hamilton RS, Hampl A, Healy LE, Hovatta O, Hyllner J, Imreh MP, Itskovitz-Eldor J, Jackson J, Johnson JL, Jones M, Kee K, King BL, Knowles BB, Lako M, Lebrin F, Mallon BS, Manning D, Mayshar Y, McKay RD, Michalska AE, Mikkola M, Mileikovsky M, Minger SL, Moore HD, Mummery CL, Nagy A, Nakatsuji N, O'Brien CM, Oh SK, Olsson C, Otonkoski T, Park KY, Passier R, Patel H, Patel M, Pedersen R, Pera MF, Piekarczyk MS, Pera RA, Reubinoff BE, Robins AJ, Rossant J, Rugg-Gunn P, Schulz TC, Semb H, Sherrer ES, Siemen H, Stacey GN, Stojkovic M, Suemori H, Szatkiewicz J, Turetsky T, Tuuri T, van den Brink S, Vintersten K, Vuoristo S, Ward D, Weaver TA, Young LA, Zhang W. Characterization of human embryonic stem cell lines by the International Stem Cell Initiative. Nat Biotechnol 2007;25(7):803–816. [PubMed: 17572666]

[30]. Chambers I, Colby D, Robertson M, Nichols J, Lee S, Tweedie S, Smith A. Functional expression cloning of Nanog, a pluripotency sustaining factor in embryonic stem cells. Cell 2003;113(5):643–655. [PubMed: 12787505]

[31]. Mitsui K, Tokuzawa Y, Itoh H, Segawa K, Murakami M, Takahashi K, Maruyama M, Maeda M, Yamanaka S. The homeoprotein Nanog is required for maintenance of pluripotency in mouse epiblast and ES cells. Cell 2003;113(5):631–642. [PubMed: 12787504]

[32]. Nichols J, Zevnik B, Anastassiadis K, Niwa H, Klewe-Nebenius D, Chambers I, Scholer H, Smith A. Formation of pluripotent stem cells in the mammalian embryo depends on the POU transcription factor Oct4. Cell 1998;95(3):379–391. [PubMed: 9814708]

[33]. Baldassarre G, Bianco C, Tortora G, Ruggiero A, Moasser M, Dmitrovsky E, Bianco AR, Ciardiello F. Transfection with a CRIPTO anti-sense plasmid suppresses endogenous CRIPTO expression and inhibits transformation in a human embryonal carcinoma cell line. Int J Cancer 1996;66(4):538–543. [PubMed: 8635871]

[34]. Vallier L, Mendjan S, Brown S, Chng Z, Teo A, Smithers LE, Trotter MW, Cho CH, Martinez A, Rugg-Gunn P, Brons G, Pedersen RA. Activin/Nodal signalling maintains pluripotency by controlling Nanog expression. Development 2009;136(8):1339–1349. [PubMed: 19279133]

[35]. Stern CD. Neural induction: old problem, new findings, yet more questions. Development 2005;132 (9):2007–2021. [PubMed: 15829523]

[36]. Westfall SD, Sachdev S, Das P, Hearne LB, Hannink M, Roberts RM, Ezashi T. Identification of oxygen-sensitive transcriptional programs in human embryonic stem cells. Stem Cells Dev 2008;17 (5):869–881. [PubMed: 18811242]

[37]. Darr H, Mayshar Y, Benvenisty N. Overexpression of NANOG in human ES cells enables feeder-free growth while inducing primitive ectoderm features. Development 2006;133(6):1193–1201. [PubMed: 16501172]

[38]. Xu RH, Sampsell-Barron TL, Gu F, Root S, Peck RM, Pan G, Yu J, Antosiewicz-Bourget J, Tian S, Stewart R, Thomson JA. NANOG is a direct target of TGFbeta/activin-mediated SMAD signaling in human ESCs. Cell Stem Cell 2008;3(2):196–206. [PubMed: 18682241]

[39]. Rodriguez RT, Velkey JM, Lutzko C, Seerke R, Kohn DB, O'Shea KS, Firpo MT. Manipulation of OCT4 levels in human embryonic stem cells results in induction of differential cell types. Exp Biol Med (Maywood) 2007;232(10):1368–1380. [PubMed: 17959850]

[40]. Niwa H, Miyazaki J, Smith AG. Quantitative expression of Oct-3/4 defines differentiation, dedifferentiation or self-renewal of ES cells. Nat Genet 2000;24(4):372–376. [PubMed: 10742100]

[41]. Hay DC, Sutherland L, Clark J, Burdon T. Oct-4 knockdown induces similar patterns of endoderm and trophoblast differentiation markers in human and mouse embryonic stem cells. Stem Cells 2004;22(2):225–235. [PubMed: 14990861]

[42]. Velkey JM, O'Shea KS. Oct4 RNA interference induces trophectoderm differentiation in mouse embryonic stem cells. Genesis 2003;37(1):18–24. [PubMed: 14502573]

[43]. Matin MM, Walsh JR, Gokhale PJ, Draper JS, Bahrami AR, Morton I, Moore HD, Andrews PW. Specific knockdown of Oct4 and beta2-microglobulin expression by RNA interference in human embryonic stem cells and embryonic carcinoma cells. Stem Cells 2004;22(5):659–668. [PubMed: 15342930]

[44]. Pan G, Li J, Zhou Y, Zheng H, Pei D. A negative feedback loop of transcription factors that controls stem cell pluripotency and self-renewal. FASEB J 2006;20(10):1730–1732. [PubMed: 16790525]

[45]. Ramalho-Santos J, Varum S, Amaral S, Mota PC, Sousa AP, Amaral A. Mitochondrial functionality in reproduction: from gonads and gametes to embryos and embryonic stem cells. Hum Reprod Update. 2009

[46]. Stern S, Biggers JD, Anderson E. Mitochondria and early development of the mouse. J Exp Zool 1971;176(2):179–191. [PubMed: 5559227]

[47]. Houghton FD. Energy metabolism of the inner cell mass and trophectoderm of the mouse blastocyst. Differentiation 2006;74(1):11–18. [PubMed: 16466396]

[48]. Finkel T. Oxidant signals and oxidative stress. Curr Opin Cell Biol 2003;15(2):247–254. [PubMed: 12648682]

[49]. Carriere A, Carmona MC, Fernandez Y, Rigoulet M, Wenger RH, Penicaud L, Casteilla L. Mitochondrial reactive oxygen species control the transcription factor CHOP-10/GADD153 and adipocyte differentiation: a mechanism for hypoxia-dependent effect. J Biol Chem 2004;279(39): 40462–40469. [PubMed: 15265861]

[50]. Thannickal VJ, Fanburg BL. Reactive oxygen species in cell signaling. Am J Physiol Lung Cell Mol Physiol 2000;279(6):L1005–1028. [PubMed: 11076791]

[51]. Chung S, Dzeja PP, Faustino RS, Perez-Terzic C, Behfar A, Terzic A. Mitochondrial oxidative metabolism is required for the cardiac differentiation of stem cells. Nat Clin Pract Cardiovasc Med 2007;4(Suppl 1):S60–67. [PubMed: 17230217]

[52]. Spitkovsky D, Sasse P, Kolossov E, Bottinger C, Fleischmann BK, Hescheler J, Wiesner RJ. Activity of complex III of the mitochondrial electron transport chain is essential for early heart muscle cell differentiation. Faseb J 2004;18(11):1300–1302. [PubMed: 15180963]

[53]. Cauffman G, Van de Velde H, Liebaers I I, Van Steirteghem A. Oct-4 mRNA and protein expression during human preimplantation development. Mol Hum Reprod 2005;11(3):173–181. [PubMed: 15695770]

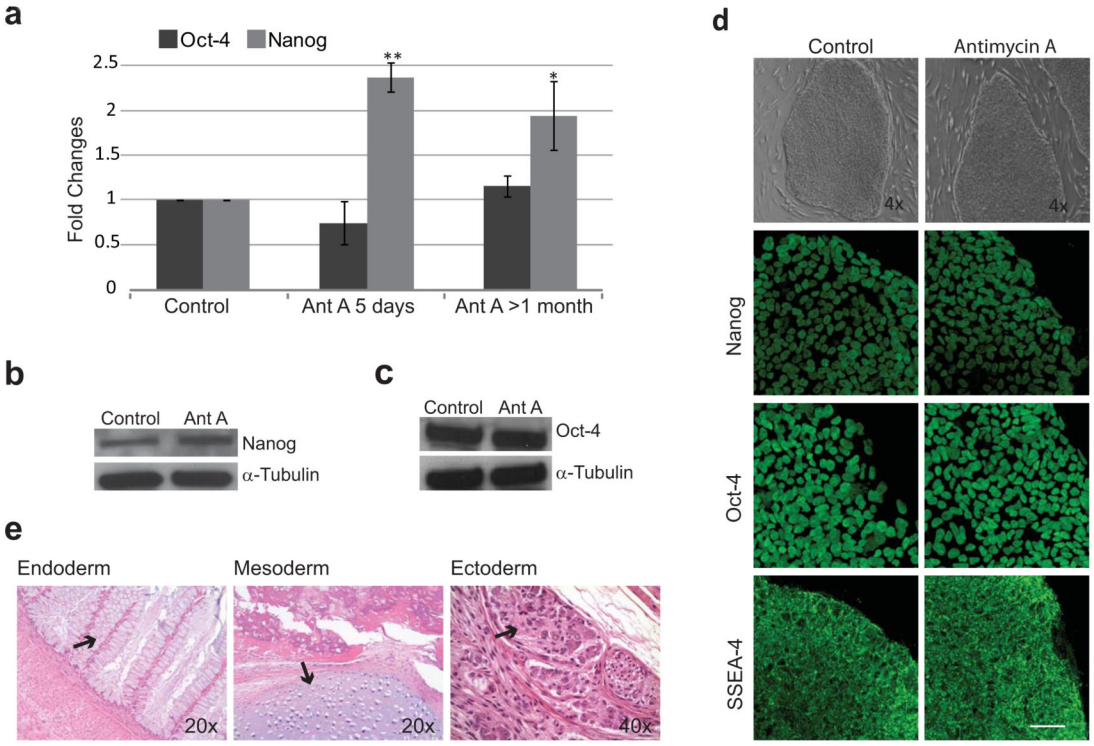

Figure 1. Analysis of Pluripotency after Antimycin A Treatment

(a) Real Time PCR for the pluripotency markers Nanog and Oct-4 in hESC treated with Antimycin A for 5 days or 4-8 passages. Statistical significant differences were determined by paired t-test; n=6 and 3 respectively. **P<0.01; *P<0.05. (b-c) Western blot analysis for Nanog and Oct-4 protein levels in hESCs treated with Antimycin A for 4-8 passages. (d) hESC morphology and pluripotency marker pattern expression after treatment with Antimycin A for 4-8 passages, examined by phase contrast microscopy, ICC and confocal laser scanning microscopy. (e) H&E staining of teratoma sections from hESC treated with Antimycin A for 9 passages. Abbreviations: Ant A, Antimycin A; Error bars, SEM. Scale bar, 50μm.

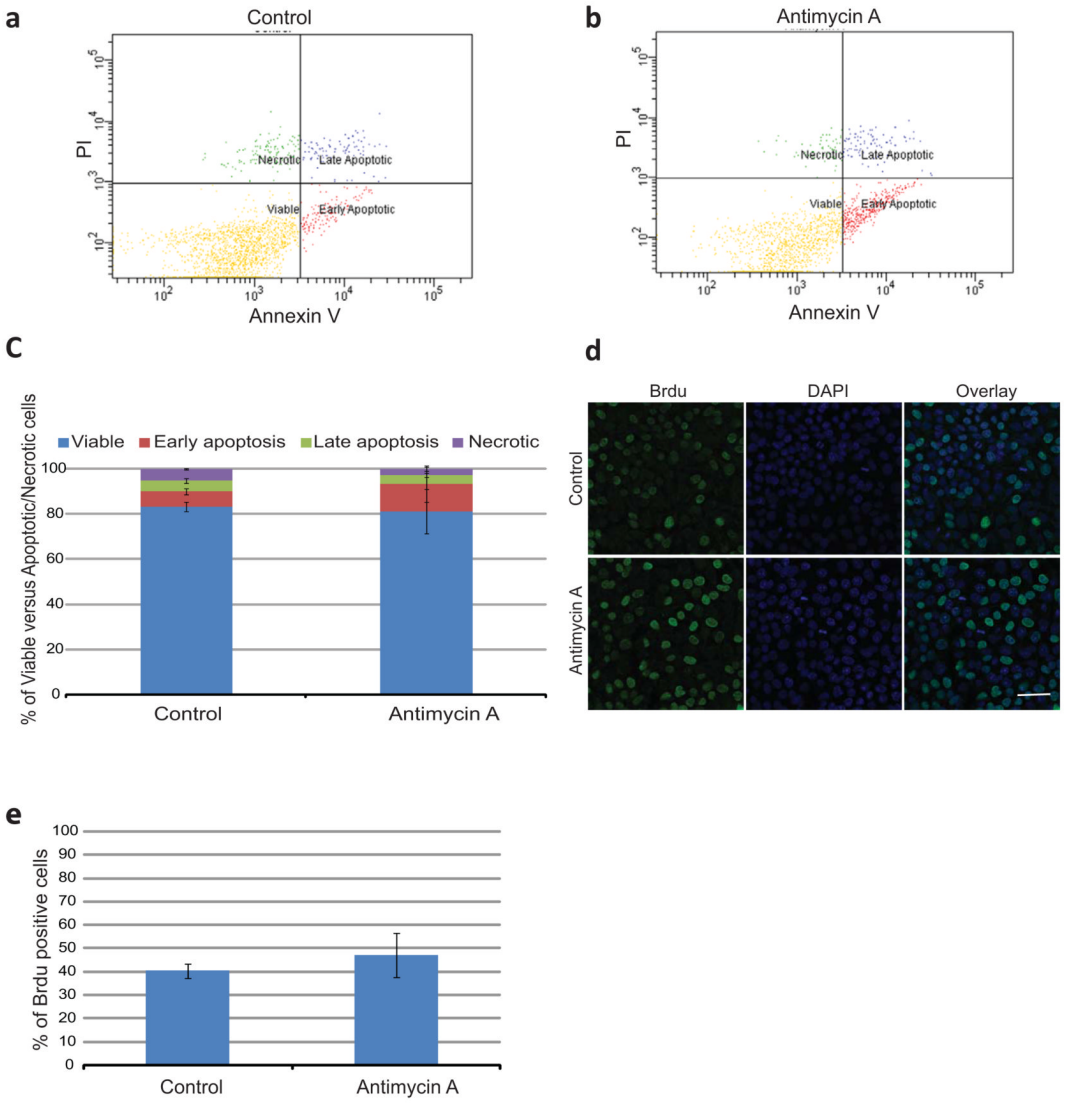

Figure 2. Analysis of Apoptosis/ Necrosis and Proliferation Rates after Antimycin A Treatment

(a-b) Representative dot plots of flow cytometry for Annexin V/PI of control and Antimycin A treated hESC. Four populations were identified: viable cells (negative for both Annexin V and PI); early apoptotic cells (positive for Annexin V and negative for PI); late apoptoic cells (positive for both Annexin V and PI) and necrotic cells (only positive for PI). (c) Percentage of the different cell populations in both control and Antimycin A treated cells (d) Brdu incorporation in both control and Antimycin A treated hESCs, examined by Confocal microscopy. (e) Percentage of Brdu positive cells. Error bars, SEM. Scale bar, 50μM

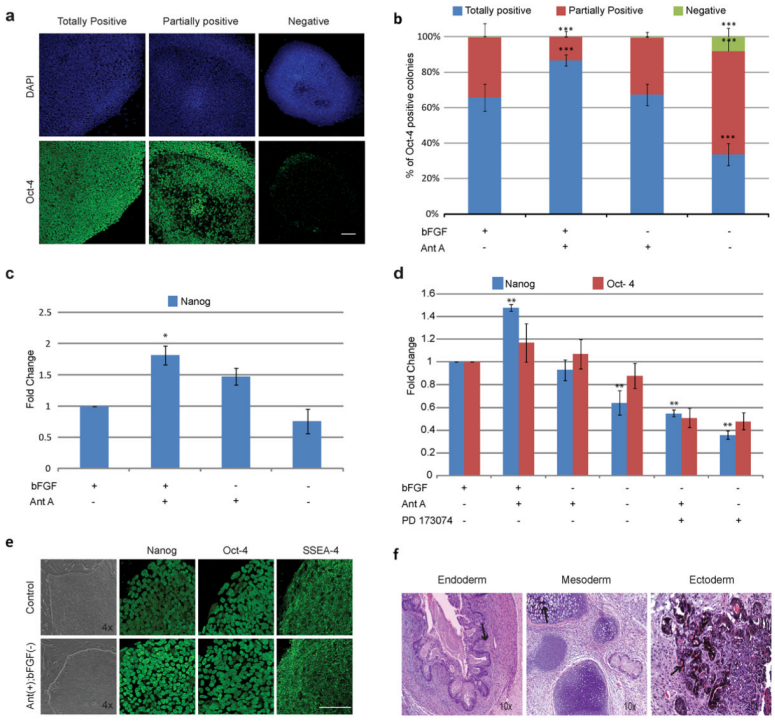

Figure 3. Analysis of Pluripotency after Antimycin A Treatment in the Absence of bFGF

(a) Oct-4 expression pattern categories in hESC analyzed by ICC and confocal laser scanning microscopy. (b) Percentage of totally positive, partially positive and negative colonies for Oct-4 in Antimycin A treated cells in the presence or absence of bFGF for 7 days. Three independent experiments were performed, and at least 200 colonies total were analyzed per condition. Statistical significance was determined by Chi-Square test ***P<0.001. (c) Real Time PCR for Nanog in hESC treated with different combinations of Antimycin A and bFGF for 7 days. Statistical significance was determined by One way ANOVA followed by Dunnet's Multiple Comparison test. *p<0.05. (d) Real Time PCR for Nanog and Oct-4 in hESC maintained on matrigel for 7 days with different combinations of bFGF, Antimycin A and PD173074. Statistical significance was determined by One way ANOVA followed by Dunnet's Multiple Comparison test. **p<0.01. (e) hESC morphology and pluripotency marker pattern expression in cells treated with Antimycin A in the absence of bFGF for 4-8 passages, analyzed as described in 1d. (f) H&E staining of teratomas from hESC treated with Antimycin A in the absence of bFGF for 33 passages. Abbreviations: Ant A, Antimycin A; bFGF, basic fibroblast growth factor; (+), present; (−), absent. Error bars, SEM. Scale bar, 100μm.

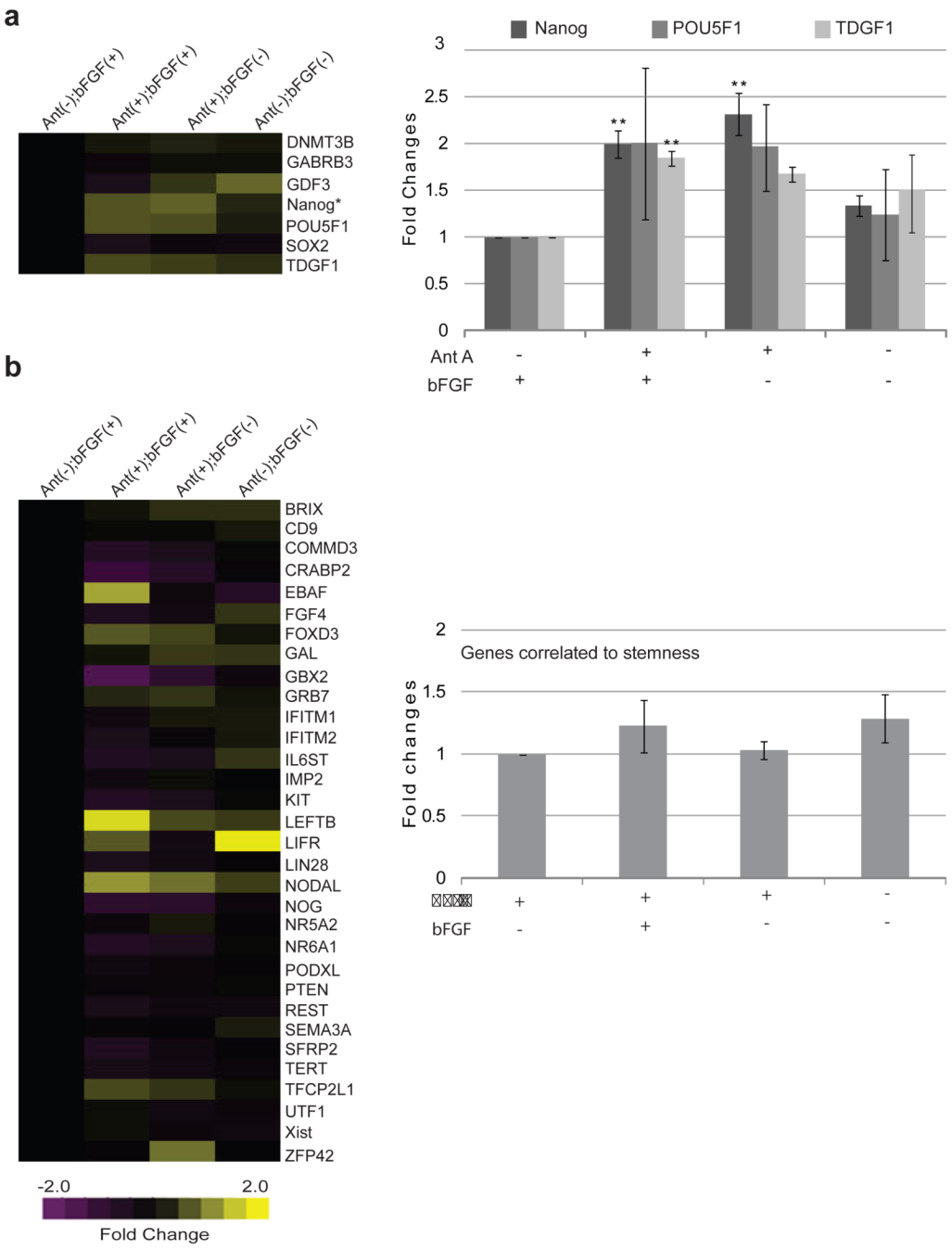

Figure 4. Pluripotency Gene Expression after Antimycin A Treatment in the Presence or Absence of bFGF

Pluripotency Gene expression profiles were analyzed by TaqMan® Array human stem cell Pluripotency Panel (a, left) Heat map for fold change differences of genes involved in the maintenance of pluripotency. (a, right) Bar graph of the fold changes differences observed for Oct-4, Nanog and TDGF1. (b, left) Heat map for genes correlated with pluripotency. (b right) Bar graph of fold change averages of genes correlated with pluripotency. In this analysis an increase in expression is represented by the yellow color, whereas a decrease is represented by the purple color. Abbreviations: Ant A, Antimycin A; bFGF, basic Fibroblast Growth Factor; (+), presence; (−), absence. Statistical significant differences were determined by One-Way

ANOVA followed by Dunnet's Multiple Comparison test. Three independent experiments were performed. Error bars, SEM. **P<0.01.

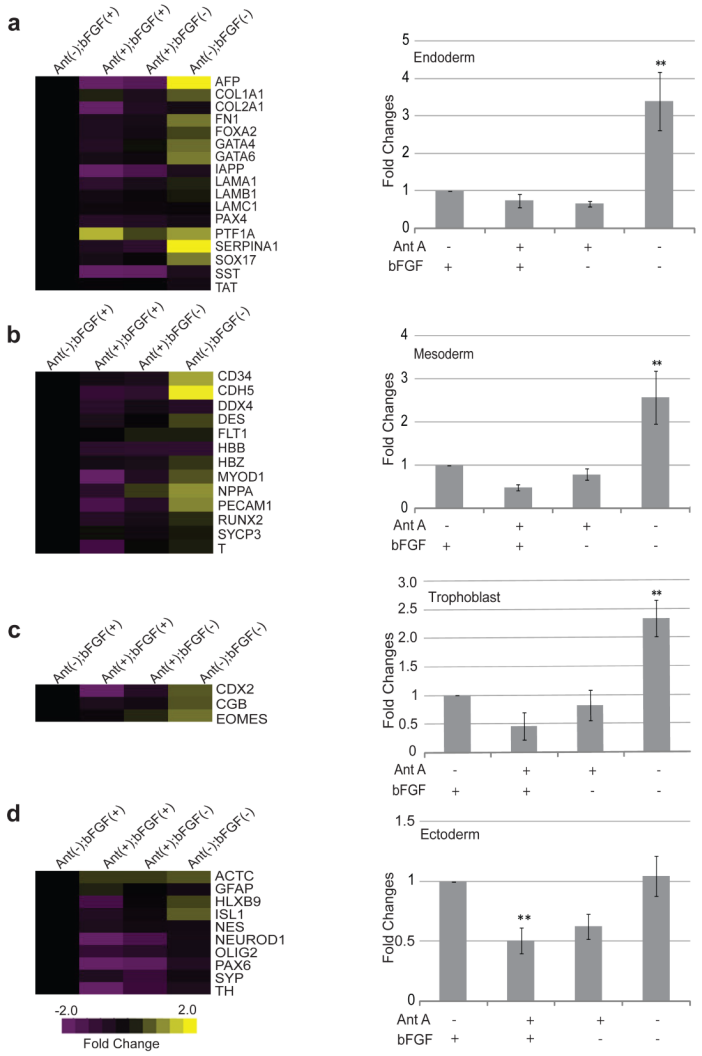

Figure 5. Differentiation Gene Expression after Antimycin A treatment in the Presence or Absence of bFGF

Differentiation gene expression profiles were analyzed by TaqMan® Array human stem cell Pluripotency Panel (a-d left) heat maps of fold change differences of differentiation genes involved in endoderm, mesoderm, trophoblast and ectoderm specification. (a-d right) bar graphs of fold changes average of differentiation genes involved in endoderm, mesoderm, trophoblast and ectoderm specification. In this analysis an increase in expression is represented by the yellow color, whereas a decrease is represented by the purple color. Abbreviations: Ant, Antimycin A; bFGF, basic Fibroblast Growth Factor; (+), presence; (−), absence. Statistical significant differences were determined by One-Way ANOVA followed by Dunnet's Multiple Comparison test. Three independent experiments were performed. Error bars, SEM. **P<0.01.

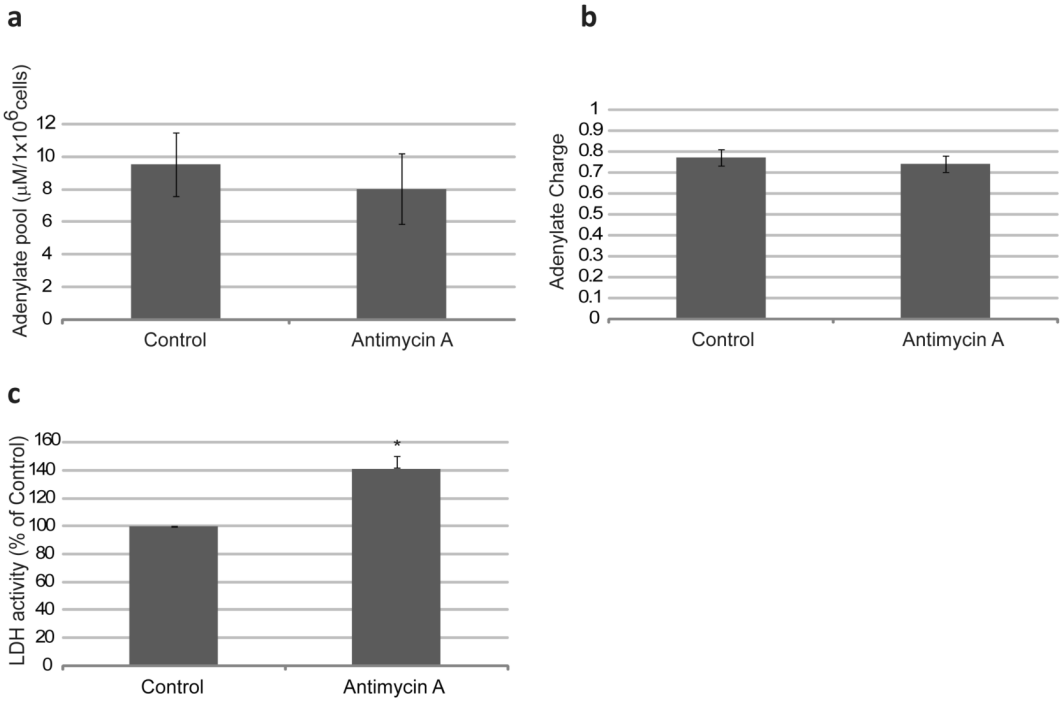

Figure 6. Energy Metabolism Analysis in Antimycin A Treated hESC

(a) Adenylate pool in Antimycin A treated cells. In order to determine the adenylate pool in the cell we performed reverse-phase High Performance Liquid Chromatography (HPLC) for ATP, ADP and AMP. (b) Adenylate Charge of Antimycin A treated cells. Adenylate energy Charge was determined according to the following formula: ATP + 0.5ADP/(ATP+ADP +AMP). (c) % of LDH activity in Antimycin A treated cells. Percentages were normalized to those found in control cells. Statistically significant differences were determined by paired t-test. Three independent experiments were performed. Error bars, SEM. *$p<0.05$.

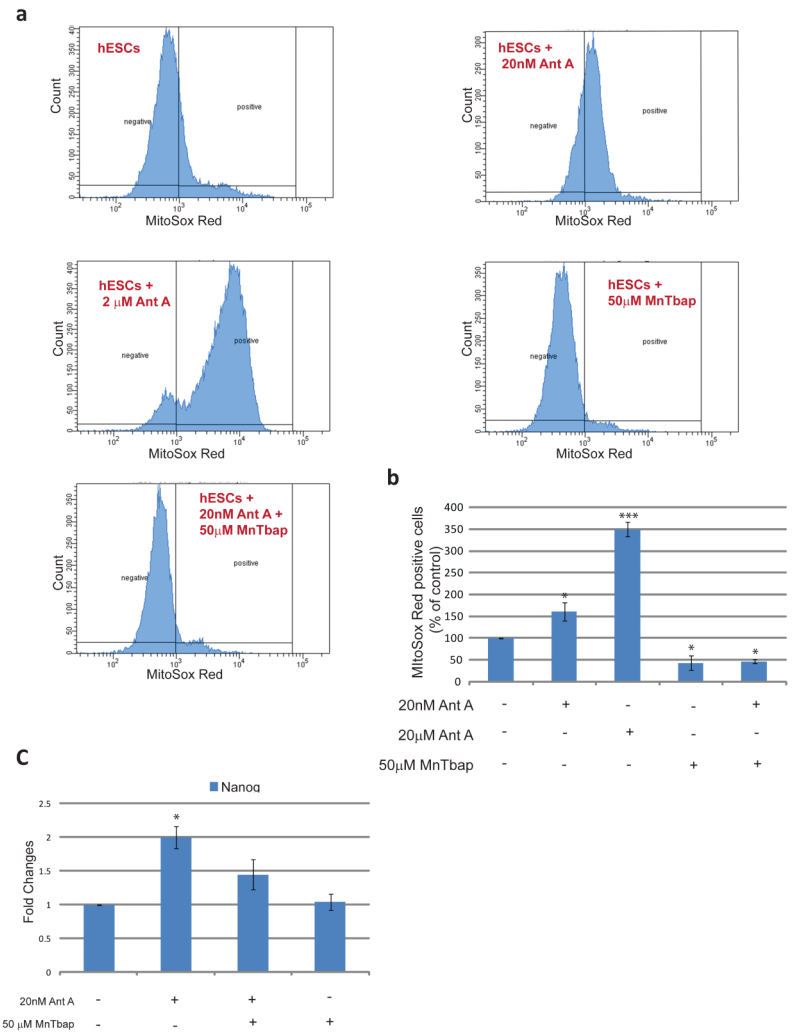

Figure7. Superoxide anion generation in Antimycin A treated hESC

(a) Representative flow cytometry histograms demonstrating percentages of MitoSox Red positive cells upon treatments with different combinations of Antimycin A and MnTbap (b) Percentages of MitoSox Red positive cells in Control *versus* treated hESCs. Percentages were normalized to those found in control cells (c) Real Time PCR for Nanog of hESCs treated with different combinations of Antimycin A and MnTbap. Statistical Significance was determined by One Way ANOVA followed by Dunnet's Multiple Comparison test. Error bars, SEM. *p<0.05; ***p<0.01